Desalination 495 (2020) 114675

Contents lists available at ScienceDirect

Desalination

journal homepage: www.elsevier.com/locate/desal

Development of a green corrosion inhibitor for use in acid cleaning of MSF desalination plant

I.B. Obot[a,*], M.M. Solomon[a], I.B. Onyeachu[a], S.A. Umoren[a], Abdelkader Meroufel[b], A. Alenazi[b], A.A. Sorour[a]

[a] Center of Research Excellence in Corrosion, Research Institute, King Fahd University of Petroleum and Minerals, Dhahran 31261, Saudi Arabia
[b] Corrosion Department, Desalination Technologies Research Institute, Saline Water Conversion Corporation, Saudi Arabia

GRAPHICAL ABSTRACT

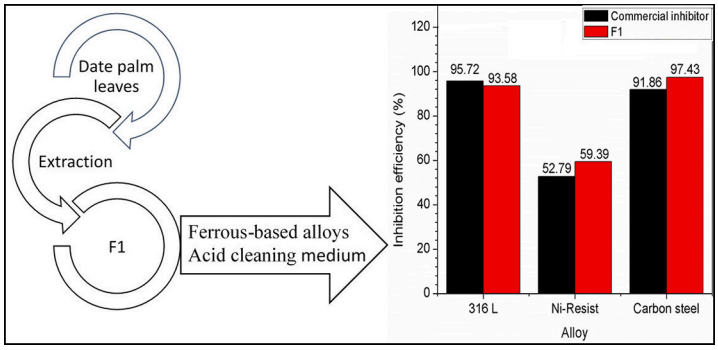

ARTICLE INFO

Keywords:
Acid cleaning
Thermal desalination
Ecofriendly
Corrosion inhibitors
Formulation

ABSTRACT

A green and cost-effective inhibitor based on Date palm leaves extract was formulated for use during acid cleaning of thermal desalination plants. The inhibitor formulation designated as F1 was tested against the corrosion of ferrous-based alloys namely: carbon steel, Ni-resist, and 316L stainless steel in 2% HCl solution at 40 °C under static and hydrodynamic conditions. Weight loss and electrochemical methods complemented with scanning electron microscopy were used in the study. Experiments were performed for 6, 24, and 72 h and the performance of F1 was compared with that of a commercial acid corrosion inhibitor. F1 exhibited excellent corrosion inhibition performance. Under static and dynamic conditions, 0.4% of F1 provided excellent corrosion inhibition up to 72 h and comparable to the commercial inhibitor performance. The inhibitors (F1 and the commercial one) exhibited a behavior typical of a mixed type corrosion inhibitor in the studied environment according to the potentiodynamic polarization. Results from cyclic potentiodynamic polarization experiments excluded pitting corrosion risk on the 316L stainless steel in the studied medium. Results from all applied techniques are in good agreement.

1. Introduction

One of the options to increase the global fresh water supply is the desalination of seawater and brackish water [1]. There are about 15,906 functional desalination plants in the world and produce about 95 million m^3/day of fresh water for human consumption [2]. Twenty

* Corresponding author.
E-mail address: Obot@kfupm.edu.sa (I.B. Obot).

https://doi.org/10.1016/j.desal.2020.114675
Received 24 June 2020; Received in revised form 29 July 2020; Accepted 31 July 2020
Available online 21 August 2020
0011-9164/

six percent of worldwide desalination plants operate based on the multistage flash (MSF) thermal desalination technique [3]. A MSF seawater desalination plant has different sections fabricated with various metallic alloys. The main components include the evaporator (carbon steels), the brine heater and evaporator condensers (Cu−Ni alloys), the ejector (stainless steels), and pump casings (Ni-resist, ASTM A439 D2 and BS 3468 S2W types) [4]. Scaling phenomenon is one of the major operational challenges affecting the long-term production performance [4]. The commonly found scales in thermal desalination plant components are the calcium carbonate, silica, calcium sulfate, metals silicates, oxides/hydroxides of Mg, and Mn [5,6]. Scaling, if not controlled would not only decrease plant production efficiency but would also promote under deposit corrosion [7,8].

Periodically, thermal desalination plants are shut down for descaling by acid cleaning process. Acid solutions, mainly hydrochloric acid, sulfuric acid, or sulfamic acid are used in the concentration range of 2–5% [4]. Sulfuric acid relative to hydrochloric acid and sulfamic acid is easy to use and is relatively inexpensive. However, the tendency of sulfate scales (especially calcium sulfate) formation is highly expected when considering sulfuric acidified seawater than in hydrochloric acidified seawater.

Acid cleaning process can induce severe corrosion of desalination plant components. It was reported [4] that, carbon steel, Cu−Ni alloys, and Ni-resist samples exposed to 2% HCl solution under atmospheric conditions for 6 h corroded at a rate of 2.56, 1.67, and 1.16 mm/yr, respectively. Meanwhile, due to the high water demand and the necessity of high level of plant availability as well as important scale if formed, acid cleaning operation may last up to 72 h. It is therefore a necessity to add an effective corrosion inhibitor to acid cleaning solutions. Organic compounds containing oxygen, nitrogen, and sulfur heteroatoms in their moiety had been studied as acid cleaning inhibitors [9–11]. Recently, Alamri and Obot [12] studied the influence of thiabendazole (TBZ) on the corrosion resistance of C1020 grade steel during acid cleaning of MSF desalination plant. It was found that, 10 mM TBZ inhibited the corrosion of C1020 steel in 1.0 M HCl by 83.30 ± 0.95% and 51.88 ± 0.79% at 25 °C and 60 °C, respectively. To enhance the corrosion inhibition performance, potassium iodide was combined with TBZ and the mixture was found to provide a synergistic effect, upgrading the inhibition efficiency to 91.67 ± 0.47% and 69.92 ± 0.45% at 25 °C and 60 °C, respectively. Propargyl ethers and propargyl thioethers had also been reported to exhibit outstanding inhibition effect toward ferrous-based alloys in acid media [13,14].

There are also information on the use of commercial corrosion inhibitors, including the quaternary ammonium salts based-IBIT 570S, aliphatic nitrogen based-ARMOHIB 28, and amine based-Nevamin CP-20 inhibitors [4,15,16] during acid cleaning of desalination plants. Although these inhibitors have been effective, some of them are expensive and harmful to human and the natural environment.

The current research direction is to develop highly efficient corrosion inhibitors with minimal toxic impacts. In view of this, Frenier [17] developed a low toxicity corrosion inhibitor based on cinnamaldehyde, quaternary nitrogen salts, and a nonionic surfactant for use in hydrochloric acid cleaning process. Static and dynamic corrosion tests revealed that the formulation provided adequate protection for a number of steels in hydrochloric acid solution at temperatures up to 150 °F without interfering in the cleaning operation. Lindert and Johnson [18] also developed a low toxicity corrosion inhibitor for use in industrial cleaning operations. As part of our contribution to this growing area of research, we formulated an inhibitor (F1) from Date palm leaves extract. The inhibiting effect of F1 was tested against carbon steel, Ni-resist, and 316 L stainless steel in 2% HCl solution under static and hydrodynamic conditions using weight loss and electrochemical techniques complemented with surface characterization by scanning electron microscope (SEM). The corrosion performance of F1 was compared with that of a commercial inhibitor recommended for use by a desalination company since 1997 [4].

Table 1
The dimensions of the coupons used for immersion test experiments.

Coupon dimension				
Coupon	Thickness (cm)	Width (cm)	Length (cm)	Area (cm^2)
Ni-resist	0.312	3.054	3.175	23.280
316 L stainless steel	0.232	3.078	3.218	22.731
Carbon steel	0.442	2.786	3.414	24.504

2. Experimental

2.1. Metals samples and preparation

In this study, ferrous corrosion coupons were chosen to represent a typical MSF alloys and include carbon steel, austenitic cast iron (Ni-resist type D2), and austenitic stainless steel 316L. The chemical composition (in wt%) of the metal samples is as follows: Carbon steel – C = 0.17, Mn = 0.83, Si = 0.10, S = 0.013, *P* = .011, Fe = balance; 316 L stainless steel – Cr = 17.03, Ni = 10.9, Mo = 2.4, C = 0.03, Si = 0.53, Fe = balance; Ni-resist – Ni = 20.76, C = 2.83, Si = 4.4, Cr = 1.96, Mn = 0.83, S = 0.004, Fe = Balance. The dimensions of the metal samples used in weight loss experiments are detailed in Table 1. The surface area of the samples was calculated using Eq. (1) [19]. Electrochemical experiment's samples were mounted in epoxy resin adopting a rectangular shape with an exposed surface area of 1 $cm^{2.}$ All specimens were grinded using SiC abrasive paper from grit #320 up to 800#. Grinding was followed by acetone degreasing, water rinsing then air drying before storage in desiccator prior to the exposure.

$$A = 2(wl + dl + dw) \quad (1)$$

where A = area (cm^2); w = width (cm); d = thickness (cm); and l = length (cm).

2.2. Corrodent and inhibitors

To mimic a typical MSF acid cleaning environment, 2% HCl solution prepared by diluting analytical grade HCl with natural gulf seawater was used as the corrodent. The chemical composition of the Jubail gulf seawater is given in Table 2 and is in accordance with the composition of the Arabian gulf seawaters given by Gouda *et al.* [20]. A desalination company provided the commercial acid cleaning corrosion inhibitor. The developed inhibitor (F1) contains ethanolic extract of Date palm leaves as the main component. Because of proprietary reason, the full composition of the corrosion inhibitor formulation, F1 will not be disclosed here. Soxhlet extractor was used for the extraction of Date palm leaves. Ten grams of sun dried and powdered Date palm leaves was extracted using 800 mL of absolute ethanol. The extract was concentrated using a rotary evaporator to a semi-solid form, which was used for the formulation. The schematic representation of the extraction procedure is depicted in Fig. 1.

Table 2
Chemical composition of Jubail gulf seawater.

Parameters	Gulf seawater (Jubail)
Na^+ (ppm)	13,400
Mg^{++} (ppm)	1603
Ca^{++} (ppm)	481
K^+ (ppm)	483
Cl^- (ppm)	23,750
SO_4^- (ppm)	3490
B (ppm)	6.2
Total suspended solids (TDS)	43,800
Total alkalinity (mg/Las $CaCO_3$)	133
pH	8.1–8.2
Conductivity (μs/cm)	61,500
Temperature (°C)	18–37

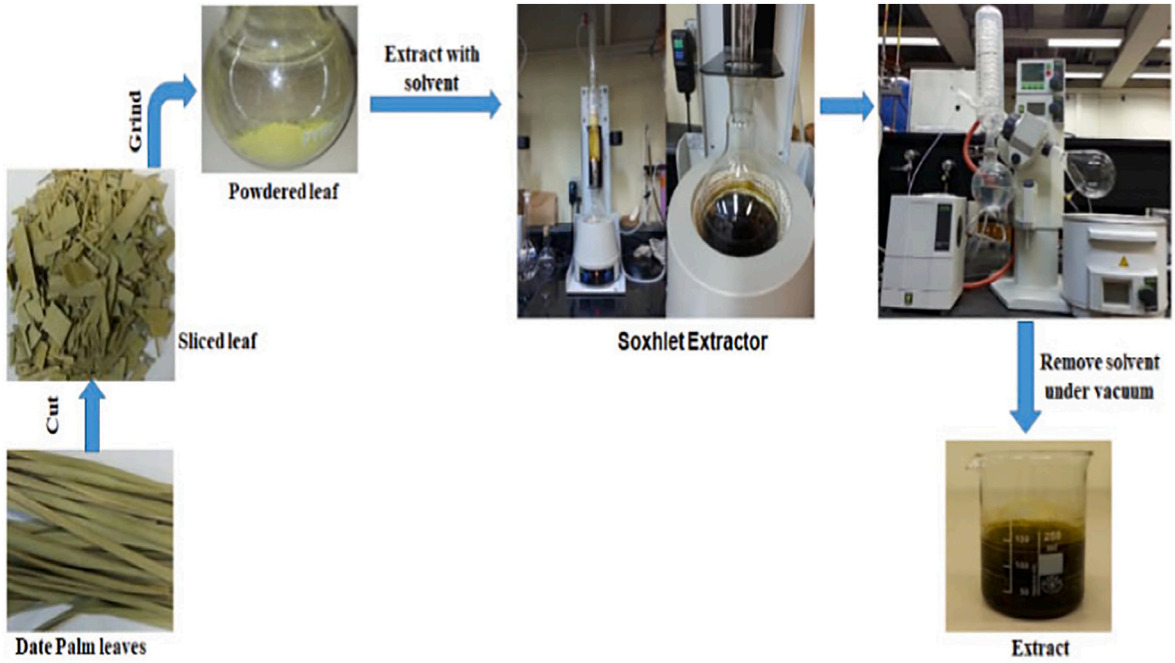

Fig. 1. Schematic representation of the extraction procedure of Date palm leaves.

2.3. Weight loss experiments

The experiments were performed under static and hydrodynamic conditions at 40 °C following the ASTM standard procedure [21]. Experiments under static condition were performed in a thermostatic water bath for 6, 24, and 72 h immersion in the test solutions. Hydrodynamic experiments were conducted for 24 and 72 h immersion under rotation speed of 415 rpm (achieved by placing the weight loss bottles on a programmable stirring hot plate model HS 65). Sample treatment after each immersion time followed the ASTM-G procedure [21] and weight loss was calculated according to Eq. (2).

$$WL\ (\mathrm{g}) = W_0 - W_1 \tag{2}$$

The corrosion rate (v) was calculated following Eq. (3) [21]:

$$v(\mathrm{mm/yr}) = \frac{87600 \times \overline{WL}}{\rho A T} \tag{3}$$

where $\overline{WL}$ = average weight loss (g), ρ = density of the steel sample (g cm^{-3}), T = immersion time (h), and A = surface area of the specimen (cm^2).

The inhibition efficiency (η%) of the inhibitor was calculated using Eq. (4) considering three concentrations: 0.3% vol./vol, 0.4% vol./vol., and 0.5% vol./vol. For simplicity, vol./vol. is omitted henceforth from the inhibitor concentration.

:

$$\eta(\%) = \frac{v_{(\mathrm{blank})} - v_{(\mathrm{inh.})}}{v_{(\mathrm{blank})}} \times 100 \tag{4}$$

where $v_{(\mathrm{blank})}$ = corrosion rate in uninhibited solution and $v_{(\mathrm{inh.})}$ = corrosion rate in inhibited solution.

2.4. Electrochemical experiments

Electrochemical tests were conducted under hydrodynamic condition at 40 °C in standard 1 L corrosion cells containing the 2% HCl solution without and with corrosion inhibitor. A Gamry 600® potentiostat was used for all electrochemical experiments including linear polarization resistance (LPR) and potentiodynamic polarization (PDP). Instantaneous corrosion rate using LPR was measured after 24 and 72 h immersion, while the PDP was conducted after 72 h immersion. Specifically, the cyclic potentiodynamic polarization (CPDP) technique (rather than the PDP) was employed for testing the 316L stainless steel in order to study pitting resistance in the presence of corrosion inhibitors as conducted by other scientists [22]. LPR tests were carried out from −10 mV to +10 mV versus open circuit potential (E_{OCP}) at the scan rate of 0.166 mV/s. PDP tests were carried out at the potential of ± 250 mV from OCP at a scan rate of 0.2 mV/s for carbon steel and Ni-resist. The CPDP tests on the stainless steel were conducted using initial potential of −250 mV/E_{OCP}, apex/reverse potential of +1000 mV/E_{OCP}, and final potential of 0 V/E_{OCP} with a scan rate of 0.2 mV/s. Prior to each experiments, the variation of E_{OCP} was monitored for 1 h to ascertain that a steady state condition is satisfied. The inhibition efficiency from LPR and PDP techniques was computed using Eqs. (5) and (6), respectively.

$$\%\eta_{\mathrm{LPR}} = 1 - \frac{R_{\mathrm{p(blank)}}}{R_{\mathrm{p(inh)}}} \times 100\% \tag{5}$$

$$\%\eta_{\mathrm{PDP}} = 1 - \frac{i_{\mathrm{corr(inh)}}}{i_{\mathrm{corr(blank)}}} \times 100\% \tag{6}$$

where $i_{\mathrm{corr\ (blank)}}$ and $R_{\mathrm{p\ (blank)}}$ are, respectively, the corrosion current density and polarization resistance recorded in the uninhibited solution; $i_{\mathrm{corr\ (inh)}}$ and $R_{\mathrm{p\ (inh)}}$ are the corrosion current density and polarization resistance recorded in the presence of an inhibitor.

2.5. Surface characterization

After 72 h immersion in the 2% HCl solution without and with 0.4% commercial inhibitor or F1, the surface morphologies of the metal coupons were observed with the aid of a scanning electron microscope (SEM) JEOL JSM-6610 LV, which was hyphenated with an energy dispersive x-ray spectrophotometer (EDAX) for determination of elemental composition.

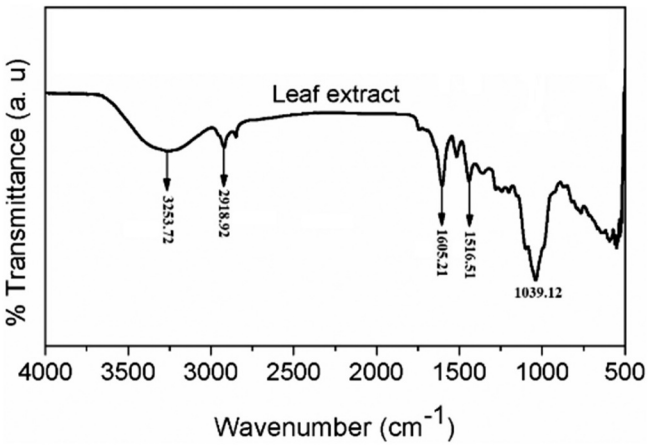

Fig. 2. ATR-IR spectrum of date palm extract.

3. Results and discussion

3.1. Characterization of Date palm extract

The ATR-IR spectrum of Date palm leaves extract acquired with the aid of an infrared reflectance spectrophotometer (PerkinElmer®, The Netherlands) is shown in Fig. 2. The wavenumber of the observed peaks and the possible assignment are summarized in Table 3. The assigned functional groups (Table 3) indicate that, the Date palm extract is rich in phytochemical compounds such as tannins, flavonoids, saponnins, alkaloids, steroids, phenols, terpenoids, carbohydrates, and amino acids, which is in agreement with previous reports [23–25].

3.2. Weight loss results

3.2.1. Corrosion inhibition performance by F1 and commercial inhibitor under static condition

Fig. 3 shows the performance of 0.4% F1 and 0.4% commercial acid inhibitor against the corrosion of three ferrous alloys exposed to 2% HCl solution for 72 h at 40 °C under static and atmospheric conditions. It is obvious from the results in the figure that both F1 and the commercial inhibitor effectively suppressed the dissolution of the alloys in the acid solution. Under atmospheric or deaerated condition, the maximum allowable corrosion rate for carbon steel and Ni-resist in inhibited HCl solution is 0.51–1.27 mm/yr (20–50 mpy) while that of stainless steel is 0.03–0.10 mm/yr (1–4 mpy) [4,26,27]. Inspection of Fig. 3(a) reveals that the studied inhibitors met the requirement.

To compare the corrosion inhibition performance of F1 with the performance of the commercial acid inhibitor, the bar chart presented in Fig. 3(b) was drawn. It is clear from the figure that F1 perform slightly better in the protection of carbon steel and Ni-resist than the commercial inhibitor. For the protection of 316 L stainless steel, F1 competes favourably with the performance of the commercial acid inhibitor. For instance, the inhibition efficiency afforded by the 0.4% F1

Table 3
FTIR result of Date palm leaves extract.

Wavenumber (cm^{-1})	Possible assignment
3253.71	O-H stretching
2918.92	C-H stretching
1743.22	C=O stretching of ester group
1605.21	C=C conjugated stretching
1516.51	C=C stretching of aromatic skeletal mode
1358.94	CH_2 bending
1244.93	C-O stretching of phenolics
1039.12	C-O stretching of polysaccharide components
569.70, 562.09	Out-of-phase CH bending and rocking

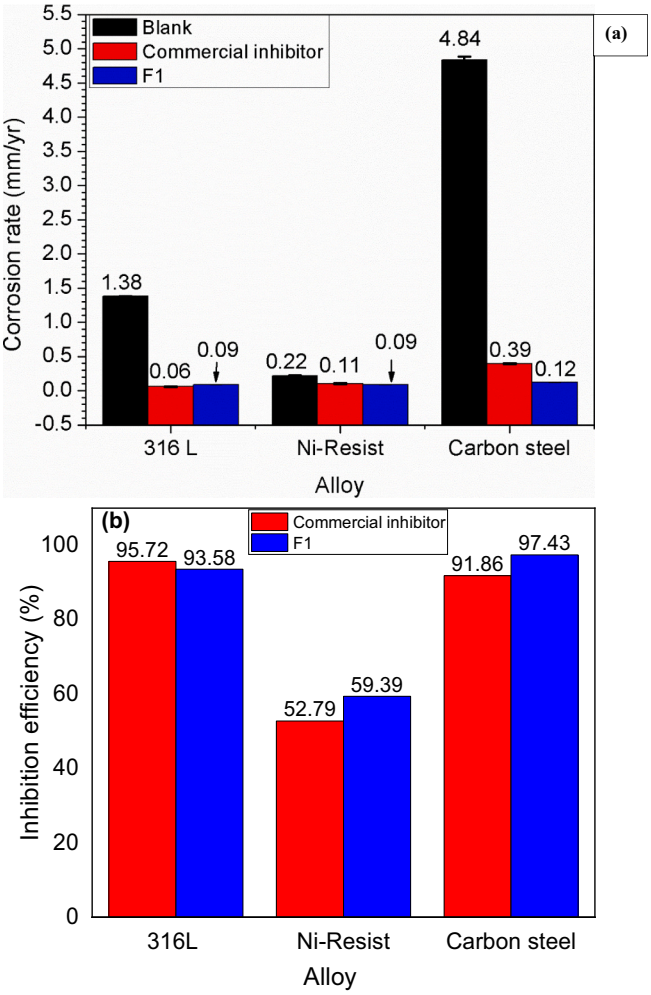

Fig. 3. Comparative bar charts showing the corrosion inhibition performance of 0.4% F1 relative to that of the commercial acid inhibitor for ferrous alloys immersed in 2% HCl solution for 72 h at 40 °C under static and atmospheric conditions.

for carbon steel and Ni-resist is 97.43% and 59.39%, respectively whereas that of the commercial inhibitor is 91.86% and 52.79%. For 316L stainless steel, inhibition efficiency of the commercial inhibitor is 95.72% while that of F1 is 93.58%. Based on these results, it could be concluded that F1 is an effective acid corrosion inhibitor for the studied ferrous alloys.

Having established that, F1 can effectively retard the corrosion of the studied ferrous alloys in HCl solution, the influence of concentration and immersion time on the performance of this green inhibitor was studied. Fig. 4 shows the variation of (a) corrosion rate and (b) protection efficiency with dosage of F1 for 316L, Ni-resist, and carbon steel immersed in 2% HCl solution for 72 h at 40 °C under static and atmospheric conditions. It is observed from Fig. 4(a) that the corrosion rate declines with increasing concentration with the lowest value observed at 0.4% concentration for carbon steel and Ni-resist and 0.5% concentration for 316L stainless steel. This observation suggests that 0.4% is the best concentration of F1 for carbon steel and Ni-resist while 0.5% is the best for 316L stainless steel. However, a careful inspection of Fig. 4(b) discloses that, the difference in inhibitive performance of the three concentrations is minimal (not exceeding 2%). For instance, the inhibition efficiency of 0.3%, 0.4%, and 0.5% F1 for 316L stainless steel is 94.42%, 93.58%, and 93.97%, respectively. Similar near constancy in inhibition efficiency with increasing F1 concentration is observed for carbon steel and Ni-resist. This implies that, the low

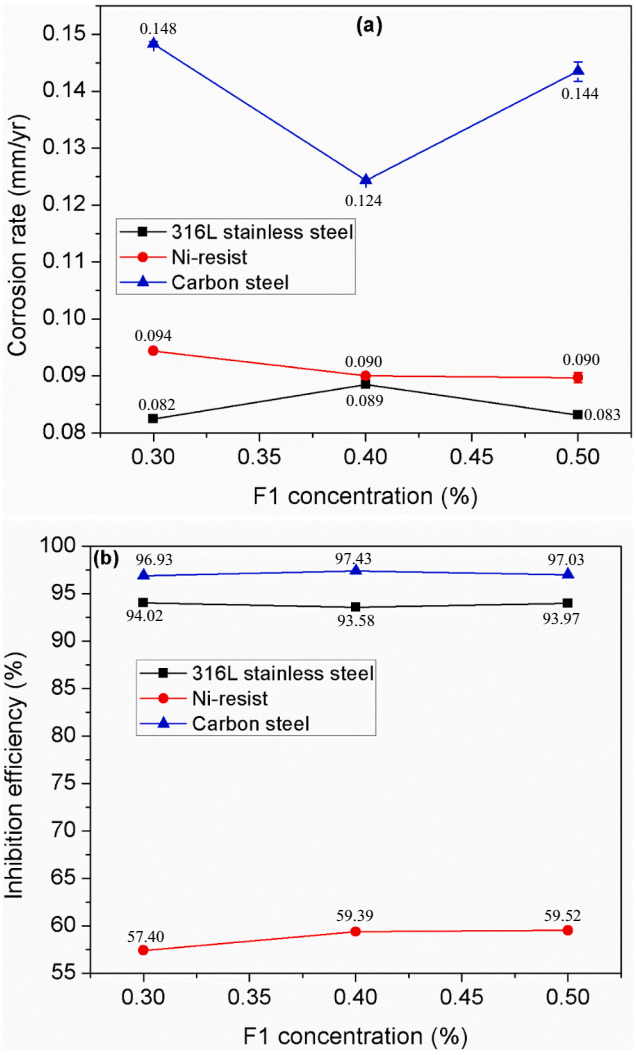

Fig. 4. Variation of (a) corrosion rate and (b) inhibition efficiency with concentration of F1 for 316L, Ni-resist, and carbon steel immersed in 2% HCl solution for 72 h at 40 °C under static condition.

concentrations of F1 (0.3–0.5%) can be utilized during acid cleaning of MSF plant to achieve desire protection of the metallic components. It should also be mentioned that the corrosion rate obtained with the three concentrations (0.3%, 0.4%, & 0.5%) of F1 for the three ferrous alloys studied falls within the acceptable limit.

Fig. 5 shows the variation of (a–c) corrosion rate and (d) inhibition efficiency of 0.4% F1 with immersion time for the studied metallurgies under the investigated experimental conditions. Beside 316 L stainless steel in which the corrosion rate in the uninhibited acid solution varies directly with immersion time (Fig. 5(a)), the corrosion rate of all other studied metals samples varies inversely with immersion time. The observed decrease in the corrosion rate with immersion time could be due to the buildup of corrosion products on the samples surfaces, which provided some degree of protection to the specimen surfaces [28]. In the other hand, the observed increase in corrosion rate of 316L stainless steel in the unprotected acid solution with immersion time suggests the breakdown of the native oxide layer at prolonged immersion duration [28].

The considerably decline in corrosion rate of the studied alloys in the inhibited systems relative to the uninhibited (Fig. 5(a–c)) further proves the effectiveness of F1 as inhibitor for the studied alloys. It does appear from the figure that the corrosion processes were inhibited at longer immersion time (*i.e* 72 h) than at shorter immersion time (*i.e* 6 h). The effectiveness of an adsorbed inhibitor layer in obstructing corrosive ions penetration depends largely on its thickness, stability, and rigidity [28,29]. It can be argued that, at longer immersion, sufficient amount of F1 molecules were adsorbed on the coupons surfaces. The adsorbed inhibitor films appreciably obstructed the ingression of the corrosive ions present in the medium and this resulted in the observed decrease in the corrosion rate. Similar argument can be found in the corrosion literature [28,29].

Three trends are observed in Fig. 5(b): first, the inhibition efficiency of F1 for 316L stainless steel increases with increase in immersion time up to 72 h. Second, for carbon steel, the performance efficiency increases up to 24 h but thereafter slightly decreases. The decline is about 1.5%, which can be considered within the measurement error range. Third, the inhibition efficiency of F1 against Ni-resist corrosion steadily decreases with increasing immersion time. Similar decline in inhibition efficiency with exposure time on cast iron and steel alloys in acidic solution had been observed by other authors [30,31]. The increase in the inhibition efficiency with increasing immersion time, as observed for stainless steel and carbon steel is attributed to an increase in the number of inhibitor molecules adsorbed on the metals surfaces [32]. In the case of Ni-resist, several factors can give rise to the observed decrease in inhibition efficiency with exposure time. First, partial desorption of adsorbed inhibitor molecules at prolonged immersion duration can cause the observed phenomenon [31]. The second possibility is that, 0.4% of F1 may not have been sufficient to overcome the fast galvanic corrosion between the cathodic carbon nodules and the anodic iron matrix in contact with the highly conductive acidic seawater.

3.2.2. Corrosion inhibition performance by F1 and the commercial inhibitor under hydrodynamic condition

Depending on its rate, flow can affect the performance of an inhibitor in three ways [33–35]: (i) increase the mass transport of inhibitor molecules from bulk solution to substrate surface. Such movement can improve the inhibition performance of an inhibitor, as more inhibitor molecules will be available for adsorption; (ii) increase the mass transport of metal ions produced during metal dissolution in corrosive medium from electrode surface to the bulk solution. In such a case, formation of metal-inhibitor complex on substrate surface will be minimal. This will have a detrimental effect on inhibition performance; (iii) cause the detachment of the adsorbed inhibitor molecules from a substrate surface in case of high shear stress caused by higher velocity.

The effect of the flow on F1 performance was investigated for an optimum concentration of 0.4% keeping the same environment conditions for a rotational speed of 415 rpm (equivalent to a velocity of 1 m/s). The experiments were performed for 24 and 72 h. The results obtained are given in Table 4. For comparison purposes, similar experiments were conducted using the commercial corrosion inhibitor. The results in Table 4 show clearly that, F1 inhibitor performed competitively with the commercial one under hydrodynamic condition. The obtained corrosion rates remain within the accepted limits. In fact, F1 performed better than the commercial inhibitor in the case of Ni-resist. This clearly shows that F1 is an effective inhibitor that can be deployed for acid cleaning process.

A comparison of the protection performance of F1 under hydrodynamic condition (Table 4) to its performance under static condition (Fig. 3) reveals better performance under static than hydrodynamic condition for carbon steel and stainless steel. The reverse is however the case with Ni-resist. For instance, the inhibition efficiency of 0.4% F1 after 72 h for carbon steel, Ni-resist, and 316L stainless steel under static condition is 97.43%, 59.39%, and 93.58%, respectively but 94.96%, 88.56%, and 88.03% under hydrodynamic condition. One or all of the factors listed above may have played a role in the observed disparity in the performance of F1 under the static and hydrodynamic conditions.

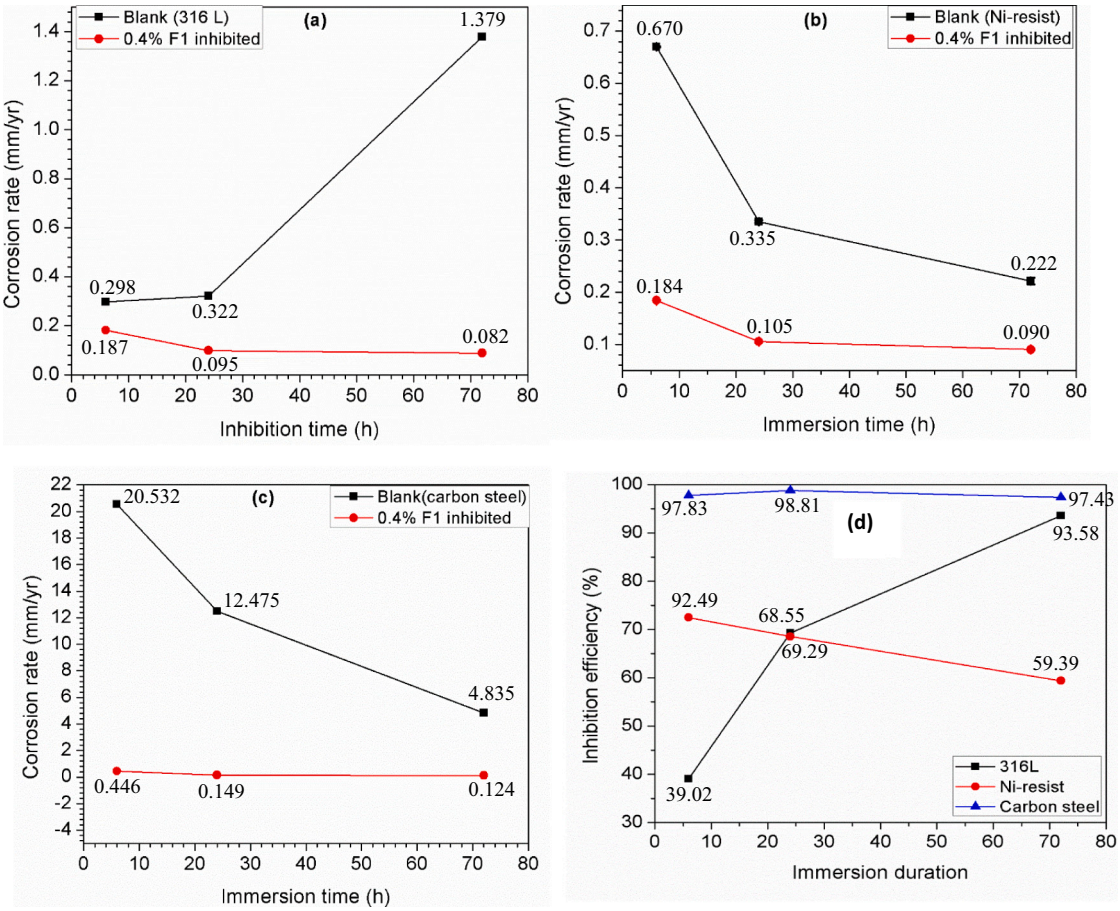

Fig. 5. Variation of (a-c) corrosion rate and (d) inhibition efficiency with immersion time for 316L, Ni-resist, and carbon steel specimens exposed to 2% HCl solution without and containing 0.4% F1 at 40 °C under static and atmospheric conditions.

3.3. Electrochemical test results

To corroborate the weight loss results and to gain insight into the mechanism of inhibition by F1 and the commercial inhibitor, electrochemical measurements were performed under hydrodynamic condition for carbon steel, Ni-resist, and 316L stainless steel immersed in 2% HCl solution for 24 and 72 h at 40 °C. Before the impedance measurements at either 24 or 72 h, the variation of open circuit potential (OCP) was monitored for 3600 s. The OCP variation collected before impedance measurements at 72 h is shown in Fig. 6.

From electrochemical perspective, an inhibitor can retard a metal corrosion by suppressing the anodic oxidation reactions or cathodic reduction reactions or both [36–38]. Most often, the extent of OCP displacement in the presence of an inhibitor relative to absent is used as a benchmark for categorizing an inhibitor as anodic, cathodic, or mixed type [36–38]. According to many authors [36–38], a precise categorization requires an OCP displacement of ± 85 mV. Inspection of Fig. 6(a) reveals that, the dominant influence of F1 and the commercial inhibitor is on the cathodic reactions. For the inhibition of Ni-resist corrosion, the inhibitors have greater effect on the anodic corrosion reactions than the cathodic (Fig. 6(b)). Fig. 6(c) suggests that, the commercial inhibitor has principal effect on the anodic dissolution of the stainless steel while F1 mainly affected the cathodic reactions. However, the displacement of the OCP by the inhibitors relative to the OCP of the blank is not sufficient to categorize F1 and the commercial inhibitor as cathodic or anodic type inhibitors. The inhibitors thus

Table 4
Performance of 0.4% commercial inhibitor and 0.4% F1 against 316L, Ni-resist, and carbon steel corrosion in 2% HCl solution at 40 °C under hydrodynamic and normal atmospheric conditions.

Conc.	Metallurgy	Average weight loss (g)		Corrosion rate (mm/yr)		Inhibition efficiency (%)	
		24 h	72 h	24 h	72 h	24 h	72 h
Blank	316 L	0.068 ± 0.007	0.719 ± 0.001	1.376 ± 0.007	4.837 ± 0.001	–	–
	Ni-Resist	0.521 ± 0.000	1.765 ± 0.009	9.800 ± 0.000	6.112 ± 0.009	–	–
	Carbon steel	1.151 ± 0.012	2.048 ± 0.042	17.620 ± 0.012	10.349 ± 0.042	–	–
F1	316 L	0.038 ± 0.000	0.086 ± 0.003	0.761 ± 0.000	0.579 ± 0.003	44.72	88.03
	Ni-Resist	0.024 ± 0.000	0.112 ± 0.002	0.460 ± 0.000	0.699 ± 0.002	95.39	88.56
	Carbon steel	0.050 ± 0.002	0.103 ± 0.001	0.761 ± 0.002	0.522 ± 0.001	95.68	94.96
Commercial inhibitor	316 L	0.028 ± 0.000	0.040 ± 0.000	0.567 ± 0.000	0.271 ± 0.000	58.80	94.39
	Ni-Resist	0.049 ± 0.002	0.137 ± 0.008	0.919 ± 0.002	0.858 ± 0.008	90.62	85.96
	Carbon steel	0.045 ± 0.003	0.103 ± 0.002	1.043 ± 0.003	1.035 ± 0.002	96.09	94.96

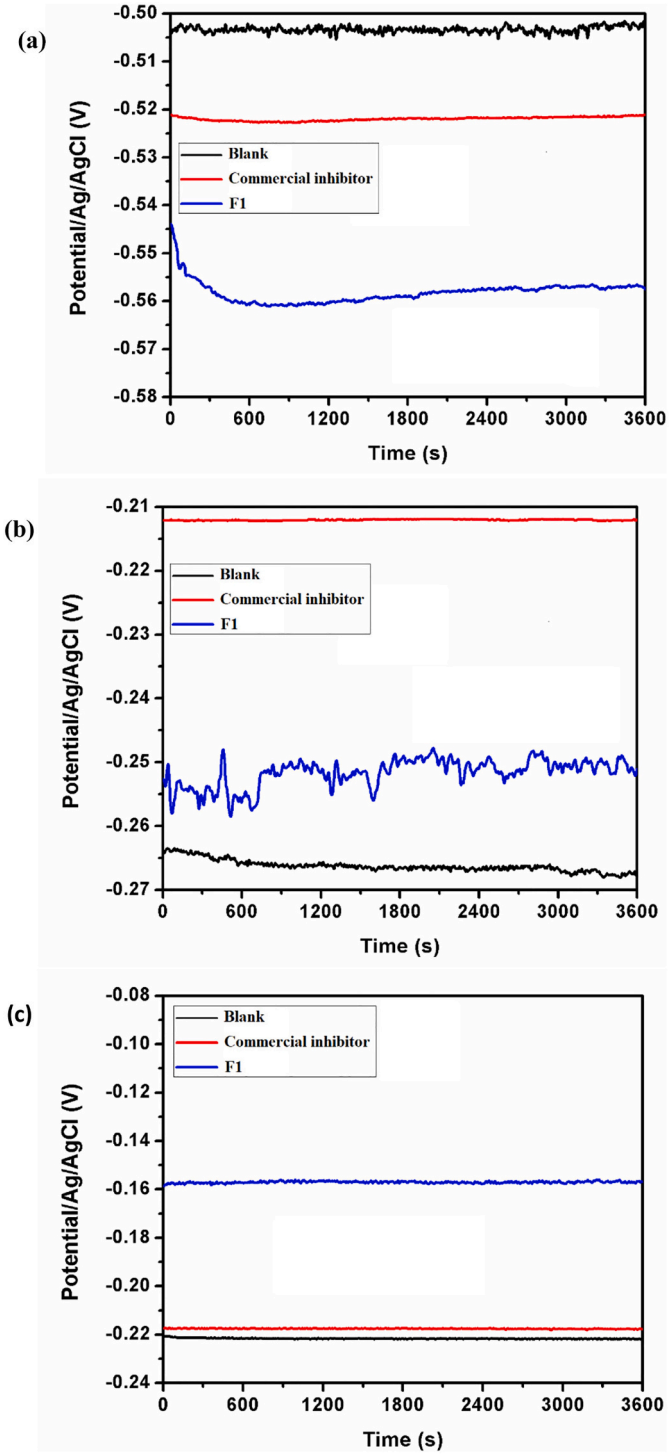

Fig. 6. OCP versus time plots for (a) carbon steel, (b) Ni-resist, and (c) 316L stainless steel exposed to 2% HCl solution without and with 0.4 vol% CP-20 and F1 under hydrodynamic condition.

behaved as mixed type inhibitors. Worthy of pointing out is the initial sharp decrease in the open circuit potential of the blank in Fig. 6(c). This may be due to the collapse of the native oxide layer on the stainless steel surface [36].

Fig. 7(a) presents the potentiodynamic polarization curves for carbon steel after 72 h of immersion in 2% HCl solution without and with 0.4% commercial inhibitor or F1 under hydrodynamic condition. The presence of the inhibitors in the acid solution caused remarkable decrease in the anodic and cathodic current densities, an indication of mixed corrosion inhibition [34]. The dominant effect is, however observed on the cathodic branch. In addition, the corrosion potential (E_{corr}) is displaced in the cathodic direction. These observations are in agreement with the OCP results (Fig. 6(a)) and support the earlier claim that the commercial inhibitor and F1 acted as a mixed type corrosion inhibitor for carbon steel but with principal effect on the cathodic half reactions.

The values of corrosion parameters derived from the polarization experiments (linear polarization (LPR) and PDP)) are presented in Table 5. In all cases, the carbon steel sample exhibited a higher polarization resistance (R_p), a lower corrosion rate (v), and a lower corrosion current density (i_{corr}) in the acid solution containing the commercial inhibitor or F1 than in their absence. Inhibition efficiency (η) of 89.6% and 96.2% was obtained for F1 from LPR and PDP, respectively. The η obtained for the commercial inhibitor from the LPR and PDP techniques is 90.5% and 96.8%, respectively. The electrochemical results (Table 5) and the weight loss results (Table 4) are comparable.

The anodic oxidation reactions of carbon steel in HCl medium proceed as follow [39,40]:

$$Fe + Cl^- \leftrightarrow (FeCl^-)_{ads} \quad (5)$$

$$(FeCl^-)_{ads} \leftrightarrow (FeCl)_{ads} + e^- \quad (6)$$

$$(FeCl)_{ads} \rightarrow FeCl^+ + e^- \quad (7)$$

$$FeCl^+ \leftrightarrow Fe^{2+} + Cl^- \quad (8)$$

The corresponding cathodic hydrogen reduction reactions follow the steps:

$$Fe + H^+ \leftrightarrow (FeH^+)_{ads} \quad (9)$$

$$(FeH^+)_{ads} + e^- \rightarrow (FeH)_{ads} \quad (10)$$

$$(FeH)_{ads} + H^+ + e^- \rightarrow Fe + H_2 \quad (11)$$

The oxidation reactions in Eqs. (5)–(8) can be interrupted in the presence of an organic-based inhibitor. Inhibitor molecules can adsorb through columbic electrostatic interactions between positively charged molecules and the negatively charged metal surface ($(FeCl^-)_{ads}$) [39,40]. The adsorbed molecules can form complexes on the metal surface through their electron pair. These layers can protect the surface from further attack by corrosive ions. On the other hand, it had been demonstrated that protonated inhibitor molecule (Inh^+) can competitively adsorb on the cathodic sites according to Eqs. (12) and (13) [39,40]. Such adsorption would abort the reactions in Eqs. (10) and (11). Since F1 and the commercial inhibitor are organic-based inhibitors (the commercial inhibitor was reported to be based on β-ethylphenylketocyclohexyl amino hydrochloride [41]), their functionalities may have been involved in the adsorption process.

$$Fe + Inh^+ \leftrightarrow Fe(Inh^+)_{ads} \quad (12)$$

$$Fe(Inh^+)_{ads} + e^- \leftrightarrow Fe(Inh)_{ads} \quad (13)$$

Fig. 7(b) shows the potentiodynamic polarization graphs for Ni-resist after 72 h of immersion in 2% HCl solution without and with 0.4% commercial inhibitor or F1 under hydrodynamic condition. Beside the fact that, both the anodic and cathodic current densities are significantly reduced, the corrosion potential is minimally displaced in the anodic direction, which are in perfect agreement with the OCP results and portray F1 and the commercial inhibitor as mixed type inhibitor with slight dominant effect on the anodic half reactions. An inspection of Fig. 7(b) discloses that, F1 inhibited the cathodic half corrosion

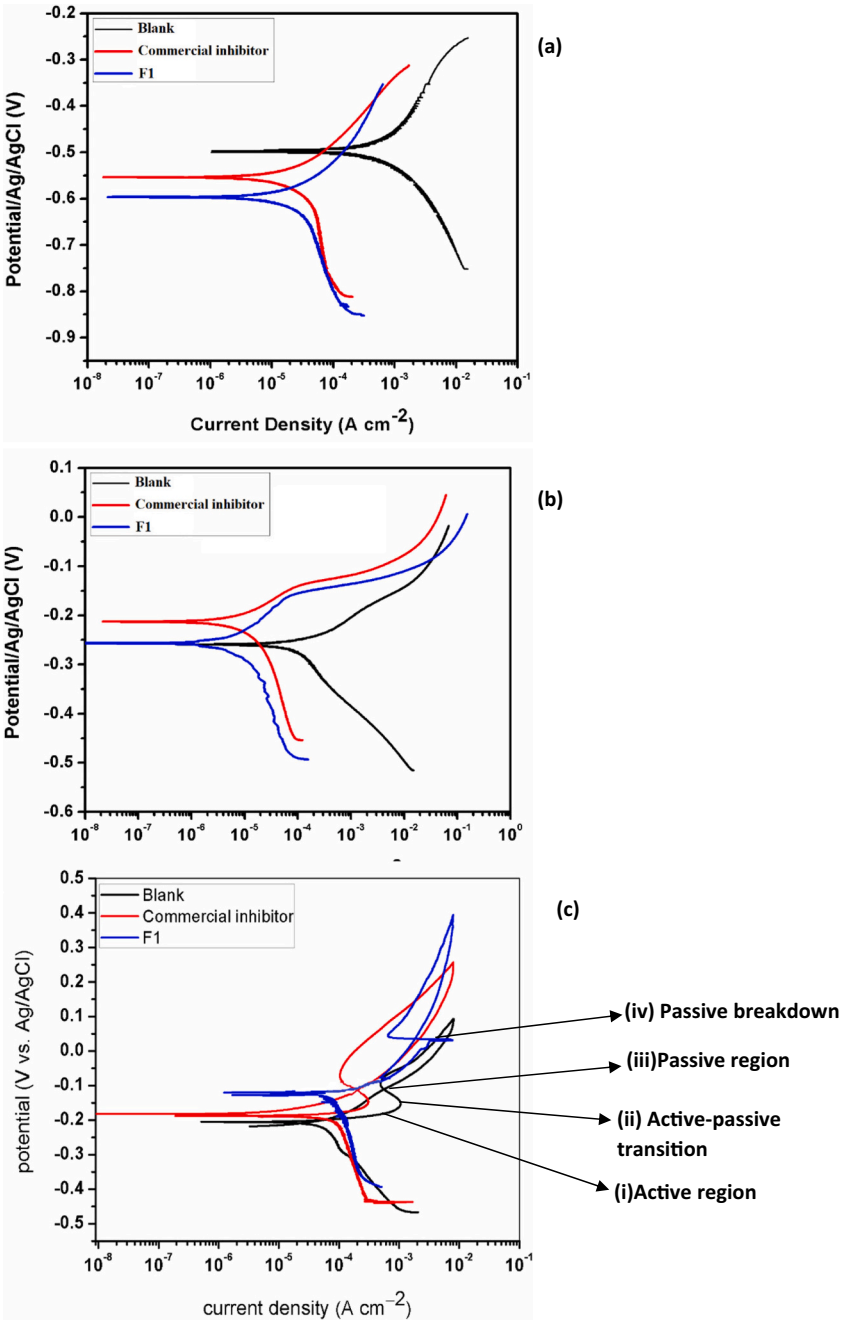

Fig. 7. Potentiodynamic polarization curves for (a) carbon steel and (b) Ni-resist; (c) cyclic potentiodynamic polarization plots for 316L stainless steel after 72 h exposure to 2% HCl solution without and with 0.4% commercial acid inhibitor and F1 under hydrodynamic condition.

reactions better than the commercial inhibitor. This seems to explain the slight better corrosion inhibition performance by F1 relative to the commercial inhibitor for Ni-resist noticed in Table 4 & 5.

Stainless steels, generally exhibit excellent corrosion resistance due to their ability to exist in a metastable of passivity [42,43]. Nevertheless, the passive layer is disrupted when stainless steels are exposed to aggressive environment containing chloride ions giving rise to pitting or crevice corrosion [42,43]. It is believed that the breakdown of the passive layer is due to potential-controlled adsorption of chloride ions on specific sites [44,45]. As such, techniques like the cyclic potentiodynamic polarization (CPDP) have been used to ascertain the resistance of a metal to localized corrosion and the extent of passivation in chloride containing environments [44].

Fig. 7(c) shows the CPDP graphs obtained for 316L stainless steel immersed in 2% HCl solution without and with 0.4% commercial inhibitor or F1 under hydrodynamic condition for 72 h. The CPDP anodic branch is characterized by an active corrosion region, where both the corrosion potential and the current density increase steadily. Beyond the active region, the current density decreases to a critical potential often referred to as the primary passivation potential or the critical potential. This decrease is due to the formation of a passive layer on the stainless-steel surface. This layer has, however been reported to be

Table 5
Electrochemical parameters derived from linear polarization and potentiodynamic polarization measurements for carbon steel and Ni-resist.

Alloy	Inhibitor	Time (h)	LPR			PDP		
			R_p (Ω cm^2)	v (mm/yr)	η_{LPR} (%)	E_{corr} (mV vs Ag/AgCl)	i_{corr} (μA cm^{-2})	η_{PDP} (%)
Carbon Steel	Blank	24	43 ± 0.51	8.89 ± 0.001	–	–	–	–
		72	104 ± 1.33	3.63 ± 0.001	–	−506	177.60	–
	Commercial inhibitor	24	936 ± 2.71	0.40 ± 0.002	95.5	–	–	–
		72	1094 ± 1.93	0.35 ± 0.001	90.5	−561	5.69	96.8
	F 1	24	818 ± 0.71	0.46 ± 0.003	94.0	–	–	–
		72	1080 ± 1.42	0.38 ± 0.002	89.6	−601	6.71	96.2
Ni-resist	Blank	24	154 ± 4.95	1.79 ± 0.030	–	–	–	–
		72	164 ± 4.24	1.64 ± 0.030	–	−247	30.47	–
	Commercial inhibitor	24	1245 ± 1.42	0.17 ± 0.002	90.5	–	–	–
		72	1772 ± 3.54	0.15 ± 0.001	90.7	−205	3.10	89.8
	F1	24	1156 ± 6.36	0.19 ± 0.002	89.4	–	–	–
		72	2424 ± 1.42	0.11 ± 0.001	93.2	−246	1.83	94.0

Table 6
Electrochemical parameters derived from cyclic potentiodynamic polarization measurements for stainless steel after 72 h.

System	E_{corr} (mV vs Ag/AgCl)	i_{corr} (μA cm^{-2})	E_{cri} (mV vs Ag/AgCl)	i_{cri} (μA cm^{-2})	E_{pass} (mV vs Ag/AgCl)	i_{pass} (μA cm^{-2})	η_{CPDP} (%)
Blank	−219	16.99	−152	1048.17	−115	501.20	–
F1	−187	7.13	+73	483.32	+85	187.45	58.0
Commercial inhibitor	−156	8.50	−124	309.12	−67	103.89	50.0

raptured in a chloride-rich environment [45]. After the passivation region, the potential further increases with increasing current density due to either the evolution of oxygen by the decomposition of water or the breaking down of the passive layer and localized corrosion [44]. Four regions are thus identified in the anodic branch: (i) active region, (ii) active-passive transition, (iii) passive region, and (iv) passive breakdown region. By comparing the CPDP graph for the commercial inhibitor and F1 to that of the blank, it is observe that, the presence of the inhibitors in the acid solution reduced the anodic current significantly at the flade potential (primary passivation potential) and enlarged the passivation zone, suggesting the formation of a stable passive layer, hence less localized corrosion [44,45].

The values of the electrochemical parameters namely, corrosion potential (E_{corr}), critical potential (E_{crit}), passivation potential (E_{pass}), corrosion current density (i_{corr}), critical current density (i_{cri}), and passivation current density (i_{pass}) derived from the analysis of the CPDP graphs are given in Table 6. The inhibition efficiency also given in Table 6 was calculated using Eq. (6). At E_{crit} and i_{cri}, the transition of the corrosion process from active to passive state takes place and at i_{pass} and E_{pass}, the anodic dissolution of the alloy undergoes a significant reduction, bringing it to a condition of near absence of corrosion [41]. These processes, as evident in Table 6 were highly favoured in the inhibited systems than in the uninhibited system. As could be seen in the table, the E_{crit}, i_{cri}, i_{pass}, and E_{pass} values of the inhibited systems are significantly lower than those of the uninhibited.

The E_{crit} and E_{corr} can be used to thermodynamically ascertain whether pitting corrosion occur or not. If the value of E_{crit} is far nobler than E_{corr} value, there is less tendency for pit initiation [43,45]. The results in Table 6 suggest that there is very low tendency of pitting initiation in the studied systems. It is pertinent to point out the very low tendency for the stainless steel to undergo pitting corrosion in the system containing F1. The E_{crit} value (+73 mV vs Ag/AgCl) is by far nobler than the E_{corr} value (–187 mV vs Ag/AgCl).

3.4. Surface analysis

Fig. 8 displays the SEM images of the studied ferrous alloys specimens obtained after exposure to 2% HCl solution without inhibitor and with inhibitors for 72 h at 40 ° C under static and atmospheric conditions. The EDAX spectra of the corrosion products and/or inhibitor films on the surfaces of carbon steel specimens exposed to test solutions are also given in Fig. 8. Similarly, the EDAX spectra of the corrosion products and/or inhibitor films on the surfaces of Ni-resist and 316L stainless steel specimens are given in Fig. 9.

As expected, the carbon steel (Fig. 8(a)), Ni-resist (Fig. 8(d)), and 316L stainless steel (Fig. 8(g)) samples exposed to the uninhibited acid solution corroded severely. Both surface damage and corrosion products are visible. For instance, the EDAX image in Fig. 8(j) and Fig. 9(a & b) suggests that, the corrosion products on the ferrous metals' surfaces were mainly oxides and chlorides based. Previous investigations [46,47] identified $FeCl_3$, FeO, and Fe_2O_3 as corrosion products of carbon steel in HCl environment.

Compared to Fig. 8(a), (d), and (g), the metal surfaces in the presence of commercial and the developed F1 inhibitors shown in Fig. 8(b, c), (e, f), and (h, i), respectively, are smoother. It is generally accepted that corrosion retardation by organic inhibitor is a quasi-substitution process in which H_2O_{ads} (adsorbed water molecules) on a metal surface is replaced by Inh_{ads} (adsorbed inhibitor molecules) [48–50]. As evident in the EDAX spectra in Fig. 8(k & l) and Fig. 9(c -f), the commercial inhibitor and F1 inhibited the metals corrosion by virtue of adsorption onto the surface. The films on the surfaces in Fig. 8(b, c, e, f, h, & i) are enriched with organic matter as indicated by the presence of C in the EDAX spectra in Fig. 8(k & l) and Fig. 9(c-f).

4. Summary and conclusion

Seawater and brackish water desalination using thermal distillation technology like the MSF technique is always accompanied by scale

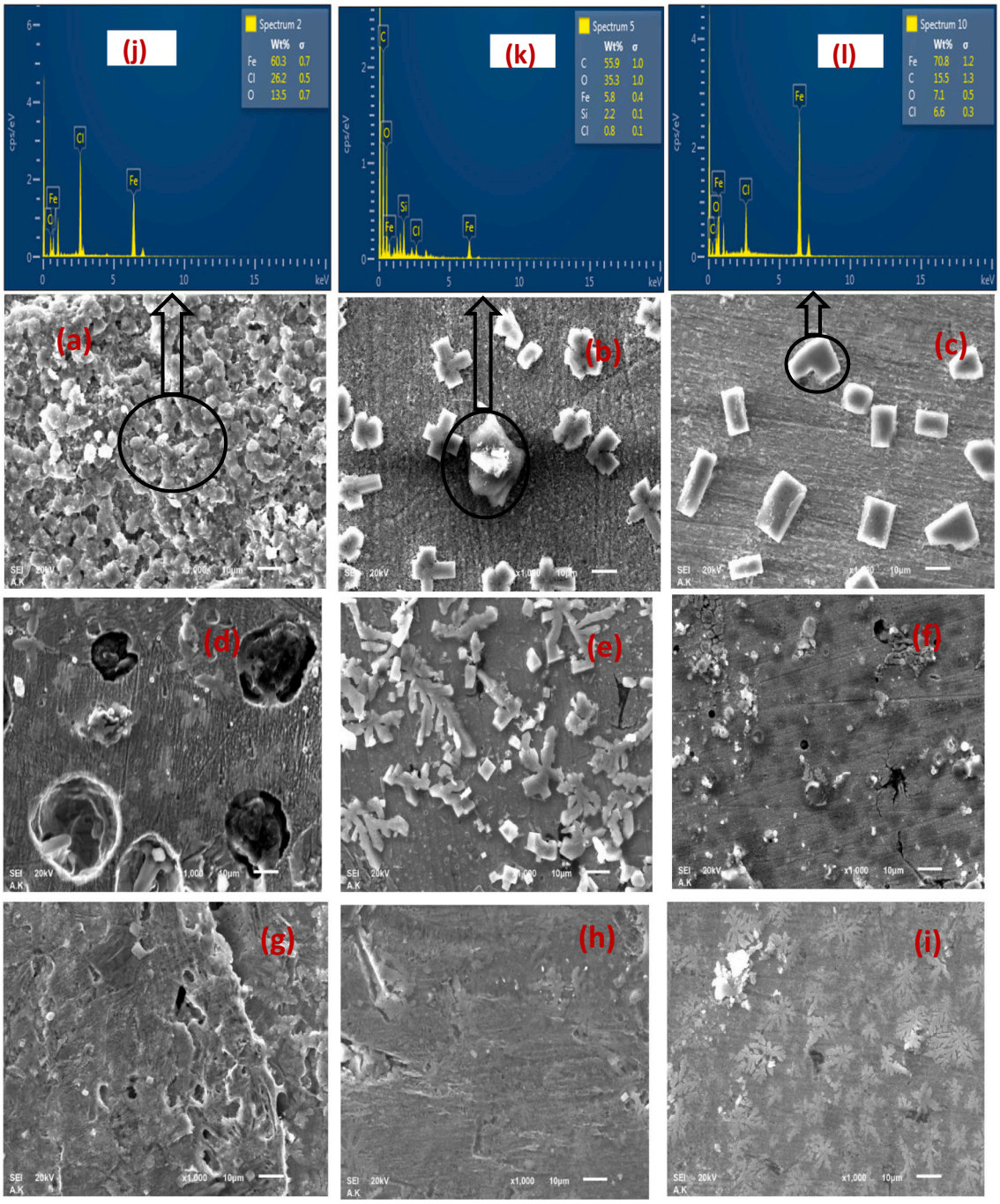

Fig. 8. SEM images of (a) carbon steel, (d) Ni-resist, and (g) 316L stainless steel specimens immersed in 2% HCl solutions without inhibitor; (b) carbon steel, (e) Ni-resist, and (h) 316L stainless steel samples images immersed in 2% HCl solutions containing 0.4% commercial acid inhibitor; (c) carbon steel, (f) Ni-resist, and (i) 316L stainless steel samples images immersed in 2% HCl solutions containing 0.4% F1 after 72 h at 40 ° C under static condition. Also shown are the EDAX spectra of products on carbon steel surface immersed (j) blank solution, (k) commercial acid inhibitor inhibited solution, and (l) F1 inhibited solution.

deposition, which is capable of decreasing the working efficiency of the plant. Acid cleaning is an important exercise periodically carried out in thermal desalination plants to remove scales. Effective corrosion inhibitors are always added to the acid solutions before used for cleaning exercise. Some of the available acid corrosion inhibitors are expensive and toxic. Effort was made to develop a cost-effective and green corrosion inhibitor from Date palm leaves extract for acid cleaning of thermal desalination plants. The formulated inhibitor (F1) was tested against the corrosion of carbon steel, Ni-resist, and 316L stainless steel in 2% HCl solution at 40 ˚C under static and hydrodynamic conditions. The performance of F1 was compared with that of a commercial acid corrosion inhibitor. Weight loss, electrochemical, and surface characterization techniques were used in the studies. F1 corrosion inhibition performance is found to be comparable to that of the commercial inhibitor. Both F1 and the commercial inhibitor act as a mixed type corrosion inhibitor for the studied substrates, inhibiting the anodic and

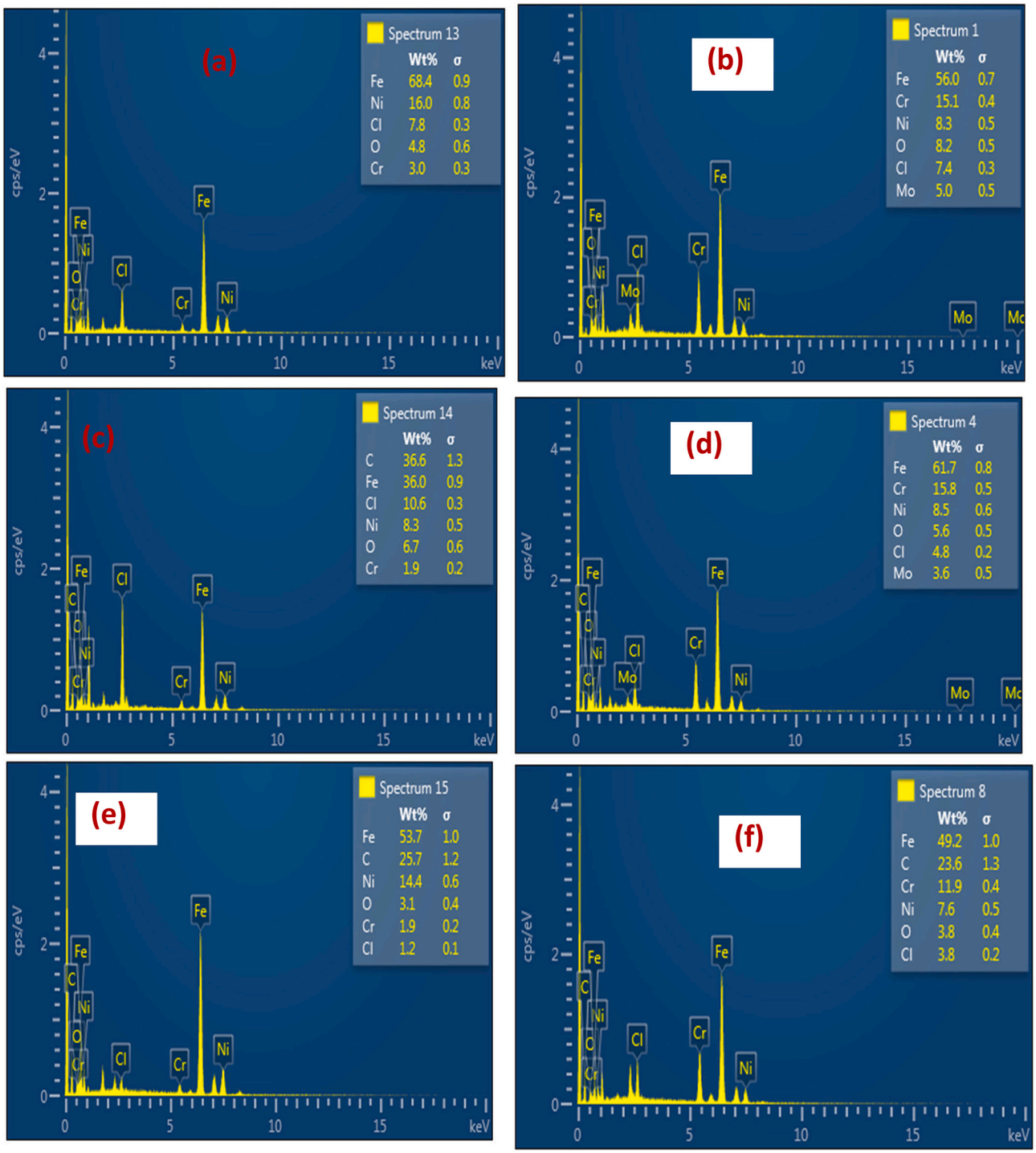

Fig. 9. EDAX spectra of products on Ni-resist and 316L stainless steel surfaces immersed (a, b) blank solution, (c, d) commercial acid inhibitor inhibited solution, and (e, f) F1 inhibited solution, respectively for 72 h at 40 ° C under static condition.

cathodic reactions. Results from cyclic potentiodynamic polarization experiments suggest no pitting corrosion of 316L stainless in the studied medium. SEM pictures reveal smoother surfaces due to corrosion inhibition by F1 and the commercial inhibitor. Results obtained from all the applied techniques are in good agreement.

CRediT authorship contribution statement

I.B. Obot designed and obtained funding for the work, analyzed the corrosion rate data and edited the manuscript. M.M.S., I.B. Onyeachu, A. A and S.A.U conducted the weight loss and electrochemical experiments. The also analyzed the results and wrote the manuscript. A.A. Sorour obtained funding and also supervised SEM and EDX analysis. A.M analyzed the corrosion rate data and edited the manuscript. All authors discussed the results and commented on the manuscript and approve final submission.

Declaration of competing interest

The authors declare no conflict of interest.

Acknowledgments

The authors would like to thank the management of the Corrosion Department at the Desalination Technologies Research Institute, Saline Water Conversion Corporation, Saudi Arabia, for funding this research work (Project No.: CREC2421) and for giving the permission to publish the findings.

References

[1] Food and Agriculture Organization of the United Nations, Coping With Water Scarcity: An Action Framework for Agriculture and Food Security, (2012) ISBN 978-92-5-107304-9.
[2] E. Jones, M. Qadir, M.T.H. vanVliet, V. Smakhtin, S. Kang, The state of desalination and brine production: a global outlook, Science of the Total Environment 657 (2019) 1343–1356.
[3] N. Ghaffour, T.M. Missimer, G.L. Amy, Technical review and evaluation of the economics of water desalination: current and future challenges for better water supply sustainability, Desalination 309 (2013) 197–207.
[4] A.U. Malik, S. Ahmad, I. Andijani, N. Asrar, Acid Cleaning of Some Desal units at Al-Jubail plant. Technical Report No. TR3804/APP95007, (February 1997).
[5] Z. Amjad, Scale Inhibition in Desalination Applications: An Overview. The NACE International Annual Conference and Exposition, Corrosion, (1996) Paper No. 230.
[6] L.A. Perez, D.M. Polizzotti, Scale Control in Thermal Desalination Processes. The NACE International Annual Conference and Exposition, Corrosion, (1999) Paper No. 110.
[7] P.G. Klepetsanis, P.G. Koutsoukos, Z. Amjad, 14th International Symposium on Industrial Crystallization, United Kingdom, Cambridge, 1999, p. 1260.
[8] F. Rahman, Z. Amjad, The Science and Technology of Industrial Water Treatment, CRC Press, Boca Raton, 2010, p. 271.
[9] A.A. Al-Hamzah, C.M. Fellows, A comparative study of novel scale inhibitors with commercial scale inhibitors used in seawater desalination, Desalination 359 (2015) 22–25.
[10] M.A. Deyab, Corrosion inhibition of heat exchanger tubing material (titanium) in MSF desalination plants in acid cleaning solution using aromatic nitro compounds, Desalination 439 (2018) 73–79.
[11] D.D.N. Singh, B. Gaur, Improving the inhibitive performance of dibenzyl sulfoxide for pickling of steel in sulfuric acid, Corrosion 51 (8) (1993) 593–601.
[12] Y. Feng, S. Chen, J. You, W. Guo, Investigation of alkylamine self-assembled films on iron electrodes by SEM, FT-IR, EIS and molecular simulations. Electrochimica Acta 53 (2007) 1743–1753.
[13] G. Schmitt, Application of inhibitors for acid media, Br.Corros. J. 19 (1984) 166–176.
[14] Japan Titanium Society, Counter measures against deposit of scale Oceanic Lives - light gauge titanium tubes for seawater desalination plants – 3, Q&A practical application (1994) 14.
[15] A.U. Malik, I.N. Andijani, A. Nadeem Siddiqi, A. Shahreer, A.S. Al-Mobayaed, Studies on the Role of Sulfamic Acid as a Descalant in Desalination Plant. Proc. VI Middle East Corrosion Conference, Bahrain, 24–26, (Jan. 1994), pp. 65–78.
[16] M.A. Deyab, Enhancement of corrosion resistance in MSF desalination plants during acid cleaning operation by cationic surfactant, Desalination 456 (2019) 32–37.
[17] W.W. Frenier, Development and testing of a low-toxicity acid corrosion inhibitor for industrial cleaning applications, The NACE International Annual Conference and Exposition, 1996 Paper No. 152.
[18] A. Lindert, W.G. Johnston, New low toxicity corrosion inhibitors for industrial cleaning operations, The NACE International Annual Conference and Exposition, 1999 Paper No. 107.
[19] ASTM-G 01–03, ASTM Book of Standards, vol. 3.02, ASTM, West Conshohocken, 2003.
[20] V.K. Gouda, I.M. Banat, W.T. Riad, S. Mansour, Microbiologically Induced Corrosion of UNS N04400 in Seawater, Corrosion 49 (1) (1993) 63–73.
[21] ASTM-G 01–03, Standard practice for preparing, cleaning, and evaluation corrosion test specimens, ASTM Book of Standards (Re-approved 1997).
[22] T. Bellezze, G. Giuliani, G. Roventi, Study of stainless steels corrosion in a strong acid mixture. Part 1: cyclic potentiodynamic polarization curves examined by means of an analytical method, Corrosion Science 130 (2018) 113–125.
[23] N. K. J. Al-Dawah, S. L. Ibrahim. Phytochemical characteristics of Date Palm (*Phoenix dactylifera* L.) leaves extracts. or Veterinary Medical Sciences 4 (1) (2013) 90–95.
[24] H.M. Al-Swaidan, A. Ahmad, 3rd International Conference on Chemical, Biological and Environmental Engineering, 20 (2011), pp. 25–32.
[25] I. Derrouiche, I.B. Marzoug, F. Sakli, S. Roudesli, Study of extraction and characterization of ultimate Date palm fibers, Adv. Mater. 4 (2015) 7–14.
[26] M.G. Fontana, Corrosion Engineering, 3rd edition, Mc Graw Hill International, 1987, p. 172.
[27] H. Uhlig, R. Revie, Corrosion and Control, 3rd edition, John Wiley and Sons, 1985, p. 13.
[28] M.K. Pavithra, T.V. Venkatesha, K. Vathsals, K.O. Nayana, Synergistic effect of halide ions on improving corrosion inhibition behaviour of benzisothiozole-3-piperizine hydrochloride on mild steel in 0.5M H_2SO_4 medium, Corrosion Science 52 (2010) 3811–3819.
[29] S.A. Umoren, M.M. Solomon, Application of polymer composites and nanocomposites as corrosion inhibitors, in: Esther Hart (Ed.), Corrosion Inhibitors, Principles, Mechanisms, and Applications, Nova Science Publishers Inc., New York, 2017, pp. 27–58.
[30] V. Rajeswari, D. Kesavan, M. Gopiraman, P. Viswanathamurthi, Inhibition of cast Iron corrosion in acid, base, and neutral media using Schiff base derivatives, J Surfact Deterg 16 (2013) 571 https://doi-org.sdl.idm.oclc.org/10.1007/s11743-013-1439-3.
[31] M. Yadav, R.R. Sinha, S. Kumar, T.K. Sarkar, Corrosion Inhibition Effect of Spiropyrimidinethiones on Mild Steel in 15% HCl Solution Insight from: Electrochemical and Quantum Studies, RSC Adv, 2015, https://doi.org/10.1039/C5RA14406J.
[32] M. Mobin, S. Zehra, R. Aslam, L-Phenylalanine methyl ester hydrochloride as a green corrosion inhibitor for mild steel in hydrochloric acid solution and the effect of surfactant additive, RSC Adv. 6 (2016) 5890.
[33] T. Douadi, H. Hamani, D. Daoud, M. Al-Noaimi, S. Chafa, Effect of temperature and hydrodynamic conditions on corrosion inhibition of an azomethane compounds for mild steel in 1 M HCl solution, J. Taiwan Inst. Chem. Eng. 71 (2017) 388–404.
[34] X. Jiang, Y.G. Zheng, W. Ke, Effect of flow velocity and entrained sand on inhibition performances of two inhibitors for CO_2 corrosion of N80 steel in 3% NaCl solution, Corros. Sci. 47 (2005) 2636–2658.
[35] J. Aljourani, K. Raeissi, M.A. Golozar, Benzimidazole and its derivatives as corrosion inhibitors for mild steel in 1M HCl solution, Corros. Sci. 51 (2009) 1836–1843.
[36] S.A. Umoren, M.M. Solomon, U.M. Eduok, I.B. Obot, A.U. Israel, Inhibition of mild steel corrosion in H_2SO_4 solution by coconut coir dust extract obtained from different solvent systems and synergistic effect of iodide ions: ethanol and acetone extracts, Journal of Environmental Chemical Engineering 2 (2014) 1048–1060.
[37] E.E. Oguzie, Y. Li, F.H. Wang, Corrosion inhibition and adsorption behavior of methionine on mild steel in sulphuric acid and synergistic effect of iodide ion, J. Colloid Interface Sci. 310 (2007) 90–98.
[38] W.A. Badawy, K.M. Ismail, A.M. Fathi, Corrosion control of Cu – Ni alloys in neutral chloride solutions by amino acids, Electrochim. Acta 51 (2006) 4182–4189.
[39] Q.B. Zhang, Y.X. Hua, Corrosion inhibition of mild steel by alkylimidazolium ionic liquids in hydrochloric acid, Electrochim. Acta 54 (2009) 1881–1887.
[40] H. Gerengi, H.I. Ugras, M.M. Solomon, S.A. Umoren, M. Kurtay, N. Atar, Synergistic corrosion inhibition effect of 1-ethyl-1-methylpyrrolidinium tetrafluoroborate and iodide ions for low carbon steel in HCl solution, J. Adhes. Sci. Technol. 30 (21) (2016) 2383–2403.
[41] I.N. Andijani, S. Ahmad, A.U. Malik, Corrosion behavior of titanium metal in presence of inhibited sulfuric acid at 50°C, Desalination 129 (2000) 45–51.
[42] A.A. Dastgerdi, A. Brenna, M. Ormellese, M. Pedeferri, F. Bolzoni, Experimental design to study the influence of temperature, pH, and chloride concentration on the pitting and crevice corrosion of UNS S30403 stainless steel, Corros. Sci. (2019), https://doi.org/10.1016/j.corsci.2019.108160.
[43] T. Bellezze, G. Giuliani, G. Roventi, Study of stainless steels corrosion in a strong acid mixture. Part 1: cyclic potentiodynamic polarization curves examined by means of an analytical method, Corrosion Science 130 (2018) 113–125.
[44] S. Esmailzadeh, M. Aliofkhazraei, H. Sarlak, Interpretation of cyclic potentiodynamic polarization test results for study of corrosion behavior of metals: a review, Protection of Metals and Physical Chemistry of Surfaces 54 (2018) 976–989.
[45] B.E. Wilde, E. Williams, The use of current/voltage curves for the study of localized corrosion and passivity breakdown on stainless steels in chloride media, Electrochim. Acta 16 (1971) 1971–1985.
[46] M.M. Solomon, S.A. Umoren, M.A. Quraishi, M. Salman, Myristic acid based imidazoline derivative as effective corrosion inhibitor for steel in 15% HCl medium, J. Colloid Interface Sci. 551 (2019) 47–60.
[47] S.A. Umoren, M.M. Solomon, S.A. Ali, H.D.M. Dafalla, Synthesis, characterization, and utilization of a diallylmethylamine-based cyclopolymer for corrosion mitigation in simulated acidizing environment, Materials Science & Engineering C 100 (2019) 897–914.
[48] E.E. Oguzie, Y. Li, F.H. Wang, Effect of 2-amino-3-mercaptopropanoic acid (cysteine) on the corrosion behaviour of low carbon steel in sulphuric acid, Electrochim. Acta 53 (2007) 909–914.
[49] B.G. Ateya, B.E. El-Anadouli, F.M. El-Nizamy, The adsorption of thiourea on mild steel, Corros. Sci. 24 (1984) 509–515.
[50] A.A. El-Awady, B.A. Abd-El-Nabey, S.G. Aziz, Kinetic-thermodynamic and adsorption isotherms analyses for the inhibition of the acid corrosion of steel by cyclic and open-chain amines, J. Electrochem. Soc. 139 (1992) 2149–2154.